F. J. HEYMANN
Senior Engineer,
Development Engineering Department,
Steam Divisions,
Westinghouse Electric Corporation,
Lester, Pa. Mem. ASME

Turbine Blade Vibration Due to Nozzle Wakes

Turbine blade vibrations due to resonance with the nozzle passing frequency have been measured and discussed with primary emphasis on the relationships between the resonant stresses and the stage flow parameters. Vibratory stresses were measured in a full admission, single-stage, impulse steam turbine test facility. The blading was shrouded into 6-blade groups, designed to bring the out-of-phase tangential modes into resonance. Some comparisons are made between measured and predicted frequencies and mode shapes. The variation of stresses, with such parameters as stage torque, velocity ratio, and mass flow, was studied by testing at eleven different operating conditions. It was found that stresses increased with torque, but less than proportionately so. It was found that stresses varied with velocity ratio in a complicated fashion, reaching a maximum and then a minimum as velocity ratio is increased. These empirical results are interpreted qualitatively in the light of available theory. It is concluded that the apparent dependence on velocity ratio may also reflect a dependence on Mach number and a dependence on the number of wakes in simultaneous engagement with a given blade. The same rotor blading was tested with two sets of nozzle (stator) blades of different sizes, and some data were also obtained at various values of axial spacing between rotating and stationary blades. The interrelationship between the effects of relative sizes and spacing between the two blade rows is discussed.

1 Introduction and Objectives

When a rotating blade traverses the nozzles or stationary blades, it encounters periodic flow nonuniformities, often broadly referred to as wakes, associated with the flow around the stationary blades. If the frequency with which these wakes is encountered coincides with a natural frequency of the blade—or of a shrouded blade group—then a resonant vibration will be excited. This phenomenon is known as "nozzle resonance vibration."

That this could occur in steam turbines had been recognized for many years, but until the 1950's relatively little attention was given to it. The excitation frequency, being a high harmonic of the running speed, was generally far above that of the well-understood lowest vibration modes. An exception was the very stiff impulse blading in the first stage of the high-pressure turbine, which could be excited by nozzle resonance in its first mode. The energy input to this vibration mode could be minimized by suitable choice of the ratio of the nozzle pitch to blade pitch. In most blades, however, the nozzle passing frequency would cause resonance only in higher and more complicated modes for which no calculation methods were at hand. Partially perhaps as a balm to cover this lack of knowledge, it was also assumed that the energy input at these high harmonics would not be sufficiently great to cause trouble.

This assumption gradually had to be abandoned when certain failures in marine turbine Rateau blades could be ascribed only to nozzle resonance vibrations. Marine turbines would be especially vulnerable, being variable speed machines in which any vibration mode is likely to come into resonance somewhere in the operating range. These failures then spurred interest in develop-

Contributed by the Power Division and presented at the Winter Annual Meeting, New York, N. Y., December 1–5, 1968, of The American Society of Mechanical Engineers. Manuscript received at ASME Headquarters, Aug. 28, 1968. Paper No. 68-WA/Pwr-1.

Nomenclature

A = coefficient of T in equations (3a) and (3c) and Fig. 11
B = coefficient of $1/T$ in equations (3b) and (3d) and Fig. 12
b = rotor blade chord
c = stator or nozzle blade chord
C = aerodynamic force coefficient
C_S = coefficient for steady force component
C_P = coefficient for fluctuating force component
$f(\omega)$ = function in equations (3a) and (3c) and Fig. 11
F = specific stress, S/T
$g(\omega)$ = function in equations (3b) and (3d) and Fig. 12
G = steam flow rate, lb/hr
K = resonant response factor, see equation (1)
M = Mach number of nozzle exit flow
p = stator blade or nozzle pitch
r = correlation coefficient
R = resultant aerodynamic force
R_S, R_P = steady and fluctuating components of R
S = representative resonant vibratory stress (measured)
$S(\omega)$ = Sears function, defined in equation (11) and Fig. 15
T = stage torque (measured at brake)
U = wheel speed (peripheral speed of rotor blade)
v = velocity ratio, U/W
V = steam velocity relative to rotor blade
V_S, V_P = steady and fluctuating components of V
W = absolute velocity of nozzle exit flow
ΔW = velocity defect in nozzle wake
$\Delta\alpha$ = flow angle fluctuation relative to rotor blade
δ = damping log decrement
θ = nozzle gaging angle
ν = nozzle passing circular frequency, $2\pi U/p$
ω = reduced frequency, defined by equations (9) and (15)
σ_E = standard error of estimate of prediction equation
σ_F = standard deviation about fitted prediction equation
σ_M = estimate of measurement error
σ_0 = standard deviation about mean
ψ = fractional stimulus, see equation (1)

ing calculation methods for predicting the frequencies and mode shapes of the higher modes which might be subject to nozzle resonance, and the stresses which might be built up as a consequence.

In 1956 Prohl and Weaver [1, 2][1] described a computer-based approach to this problem which yields frequencies, mode shapes and stresses for shrouded groups of untwisted blades. A similar calculation method was developed by the writer's company. It was soon found, however, that this could not remain the last word, for some blades failed in which the nozzle resonance stresses calculated by that method were thought to be at a safe low level.

It was partially in order to resolve this discrepancy that an experimental program to investigate nozzle resonance vibrations came to be initiated. One specific aim of the program was to verify the existence and the character of the out-of-phase tangential modes of vibration, the so-called "bow-legged modes." In shrouded impulse blading of medium length, these are the modes which were predicted by the new calculations to come into nozzle resonance at or near full-speed conditions. A second aim of the tests was to throw as much light as possible on the nozzle resonance phenomenon, and on the validity of the various components of the calculation procedure.

It should be emphasized that the calculation method in question concerned itself with calculating the vibratory response of the blading to an *assumed* excitation, represented as a sinusoidal variation in the steam force "field" through which the blades travel. It does not attempt to calculate what this excitation magnitude would be. The problem of analyzing the unsteady aerodynamic interaction forces between moving blade rows has been tackled by Kemp and Sears [3, 4] and others [5–7], but of necessity these have had to make do with flat-plate airfoil theory, which provides a reasonable approximation to gas turbine compressor blading but not to the strongly cambered blade and nozzle sections of steam turbine impulse stages.[2] For steam turbines, therefore, the magnitude of the excitation forces has had to be deduced from experience and experiment.

For this reason, particular emphasis in the investigative program was placed on attempting to determine and to explain the dependence of vibratory stresses on operating variables of the turbine stage, such as torque, mass flow, velocity ratio, and axial spacing between stationary and rotating blades. It is this phase of the investigation with which this paper is concerned.

2 Calculation Method

The computation method used to predict the vibrational characteristics and resonance stresses, of shrouded blade groups subjected to nozzle resonance, was in most essentials similar to that described in references [1] and [2]. We shall restrict ourselves here to listing the final equation for the resonant vibratory stress amplitude at a particular blade location in a particular mode. This can be written as

$$\sigma_v = \sigma_s \psi \frac{\pi}{\delta} K \bar{\sigma} \tag{1}$$

The meaning of the symbols is as follows:

σ_s = steady stress at the base of each blade due to the mean steam force. This is, of course, proportional to the torque of the turbine stage.

ψ = "fractional stimulus," or ratio of the fluctuating component of steam force to the steady component or mean steam force on the blade. This must be specified independently; Weaver and Prohl [2] have pointed out that it may "vary in some manner (not yet known) with . . . the flow conditions of the stage."

δ = "log decrement" representing the blade group damping. This also must be independently specified.

K = "resonant response factor." This quantity is one of the outputs of the computation procedure, and relates to the efficiency with which the unsteady force field, through which the blade group travels, can transfer energy to the vibratory motion of the blade group at resonance. This depends on the mode shape of the blade group, and also on the ratio of the blade spacing or pitch to the spacing of the flow nonuniformities which provide the excitation, i.e., to nozzle pitch or some submultiple thereof.

$\bar{\sigma}$ = a stress distribution factor which relates the stress at some specific location to a reference stress for the blade group in the particular mode. This also is an output of the computation procedure.

For the purposes of this study, the "predicted stresses" of the test blading were calculated by the foregoing method and with the assumption that the fractional stimulus ψ and the log decrement δ had constant values. If this were true, the resonant stresses would be proportional to stage torque and independent of other operating variables.

One of the significant findings of this test program was that this assumption is not justified and that vibratory stresses vary greatly with other operating conditions, even when torque remains constant. Furthermore, stresses do not vary proportionately with torque even when other independent conditions are maintained constant. Either ψ or δ, or both, must therefore be recognized as variables which depend on operating parameters.

3 Test Facility and Procedure

The test facility, shown in Fig. 1, consisted of a single-stage full admission impulse turbine driving a water brake. Standard marine Rateau blading sections were used for stationary and rotating blades, but the lengths were chosen to obtain the desired blade characteristics and to suit the test facility limitations. The 162 rotating blades were straight, untapered, of 0.787-in. nominal width and 2.5-in. height, on a 25-in. root diameter. They were attached to the disk by axial "Christmas-tree" roots and were riveted at their tips to shrouds, forming 27 six-blade groups.

The majority of tests were run with a nozzle diaphragm of 70 nozzle blades of nominal width (axially) of 1.25 in. and about 18 percent gaging. An auxiliary series of tests was run with an alternate nozzle diaphragm containing 126 nozzle blades of 0.75-in. nominal width and about 17 percent gaging. Table 1 summarizes some of the predicted modes of vibration of the rotating blades, and the running speeds at which these would come into resonance with the nozzle wake frequency. The five out-of-phase tangential modes are of principal interest; the blading was designed to bring them into nozzle resonance near full-power conditions.

The reason for the alternate diaphragm was two-fold: It would provide an alternate geometry with which nozzle resonance would occur at much lower rpm and in which the K-factors would be different, and it would help in generalizing correlations of stresses with operating conditions.

Seventy-two of the blades were strain-gaged in various locations, and a slip-ring arrangement permitted 12 gage signals to be taken out and observed or recorded at any one time. The bulk of the data used for the correlations to be described in this paper, however, came from one strain-gaged group of six blades. Statistical analysis of data obtained from other blade groups as well suggested that the inherent "group-to-group" variation was not very great.

The test procedure usually consisted in setting the "nominal"

[1] Numbers in brackets designate References at end of paper.

[2] Since the writing of this manuscript, several additional papers of some relevance have appeared [15–17]. In particular, Giesing [15] deals with the interaction between two airfoils of arbitrary shape, and suggests that the method could be extended to deal with the interaction between rotor and stator cascades.

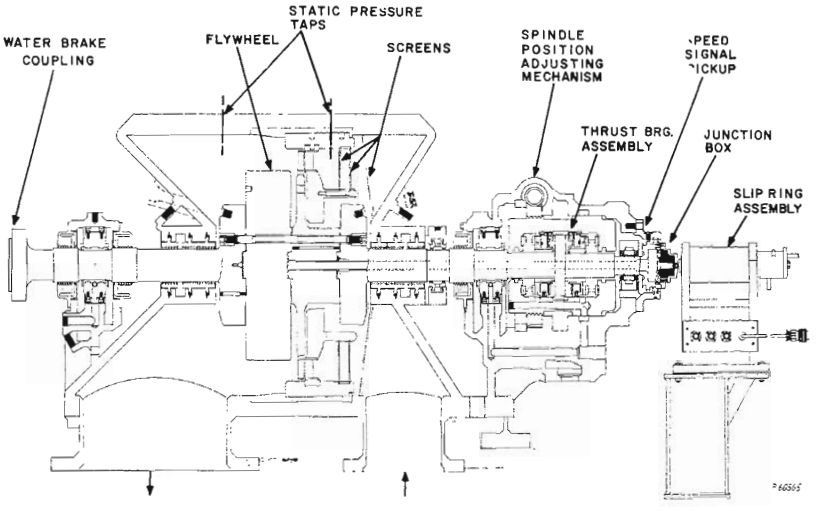

Fig. 1 Longitudinal section of test turbine

Table 1 Calculated data on modes of vibration of test blading

DESCRIPTION OF MODE	FREQUENCY Hz	MODE SHAPE	WITH 70 NOZZLES		WITH 126 NOZZLES	
			RESONANT RPM	RESPONSE FACTOR K	RESONANT RPM	RESPONSE FACTOR K
1ST IN-PHASE TANGENTIAL	1505	+ + + + + +	1290	0.970	716	0.146
1ST IN-PHASE AXIAL	1534	+ + + + + +	1313	0.158	730	0.218
1ST AXIO-TORSIONAL	2074	+ + + - - - (# #)	1780	0.080	987	0.110
1ST OUT-OF-PHASE TANGENTIAL	5923	+ - + - + - (# #)	5077	0.080	2820	0.035
2ND OUT-OF-PHASE TANGENTIAL	6018	+ - - - - + (# #)	5158	0.092	2866	0.049
3RD OUT-OF-PHASE TANGENTIAL	6109	+ + - + - - (# #)	5236	0.092	2909	0.006
4TH OUT-OF-PHASE TANGENTIAL	6205	+ - - + + - (# #)	5319	0.003	2955	0.086
5TH OUT-OF-PHASE TANGENTIAL	6213	+ + - - + + (# #)	5325	0.019	2958	0.098
2ND AXIO-TORSIONAL	6331	+ - - - - + (# #)	5427	0.045	3015	0.098

= MOST HIGHLY STRESSED BLADES

Table 2 Nominal operating conditions

CONDITION NO.	CONDITIONS FOR 70 NOZZLE OPERATION					CONDITIONS FOR 126 NOZZLE OPERATION			
	INLET PRESSURE PSIG	INLET TEMPERATURE °F	TORQUE LB-FT	FLOW LBS/HR 10^3 X	ISENTR. VELOCITY RATIO	INLET PRESSURE PSIG	TORQUE LB - FT	FLOW LBS/HR 10^3 X	ISENTR. VELOCITY RATIO
1	40	375	940	98	0.5	36	940	80	0.34
2	32	360	420	75	0.64	30	420	61	0.43
3	27.5	360	730	75	0.5	25	730	61	0.34
4	25	370	940	75	0.43	21	940	61	0.29
5	16	370	940	58	0.38	13	940	47	0.26
6	14	350	260	45	0.64	15	260	37	0.43
7	10	350	420	45	0.5	8	420	37	0.34
8	9.5	350	580	45	0.43	7	580	37	0.29
9	9	370	940	45	0.33	6	940	37	0.22
10	3	350	420	33	0.43	0	420	27	0.29
11	4" vac	350	420	28	0.38	7.5" vac	420	23	0.26

Note 1: Inlet pressure, temperature, and torque were set by test operator to above specifications.

Note 2: Some supplementary conditions were used with 126 nozzles.

operating conditions at a speed near or in the range of nozzle wake resonances, and then making "traverses" through this speed range so that one after the other of the out-of-phase tangential modes would be brought into full resonance. A speed-changing governor could automatically increase or decrease the running speed at a preset rate. The strain-gage and speed signals were recorded on a 14-channel tape recorder, and subsequently the tapes were transcribed onto a chart record which depicted the vibratory stress amplitudes directly, as well as the speed. Since the speed varied almost linearly with time, this record became in effect a stress versus speed trace, or resonance curve.

From this record the individual modes could be recognized and tabulations were made of the maximum stresses in each blade at each mode. These tabulations then formed the basis for the analyses to follow.

In order to permit correlations between stresses and operating variables, a set of 11 nominal operating conditions were selected for the 70-nozzle configuration, and a different but somewhat analogous set of conditions for the 126-nozzle configuration. This difference was necessitated by the requirement that the two configurations be operated in their respective speed ranges for nozzle resonance. The nominal operating conditions are described in Table 2.

4 General Results

The general results—relating to the identification of mode resonances, to the comparisons between stresses in different blades (i.e., mode shapes) and in different modes, and to the comparisons between absolute measured and predicted stresses—provided many interesting points of agreement as well as disagreement with the calculated predictions. In this paper these results can only be briefly summarized. All the remarks which follow refer, of course, to the five "out-of-phase" tangential modes of vibration, whose predicted frequencies ranged from 5923 to 6213 Hz, typically quite a narrow range.

First we shall list some of the apparent inconsistencies and anomalies which complicated the problem of data interpretation. Some of these have not yet been completely explained.

1 Stresses often remain high over a considerable speed range, rising to occasional stress "peaks" which are sometimes quite indistinct, rather than forming narrow independent resonance curves. This suggests that the damping is higher than was assumed, resulting in broad resonance peaks which merge into each other.

2 In a given blade, the stress peaks do not always occur at the same speed, nor are always the same number of stress peaks exhibited under different operating conditions. Not all blades in a group always exhibit stress peaks simultaneously, and not all blades in a group exhibit the same number of stress peaks.

3 The relative stress magnitudes among the various blades of a group do not agree with predictions, and are not even "symmetrical" as the predicted mode shapes invariably are. (That is, the stress amplitudes in blade No. 1 should be the same as in blade No. 6, those in blade No. 2 the same as in blade No. 5, etc., for a six-blade group.) Nor do the phase relationships between different blades fully agree with predictions. These, and the points previously listed under (2), could also be explained on the basis of damping which is high enough for the resonance curves to overlap substantially so that at any speed within the overall range of resonances two or more modes may be simultaneously excited. The observed stresses and phase relationships would then be determined by the superposition of the individual responses of several modes and not merely by that mode which is peaking.

4 The stress signals as seen on the scope often exhibit an apparent modulation of from one to about six times per revolution, and up to 100 percent of maximum amplitude. This can partially be accounted for by assuming the same mode to be excited simultaneously by more than one harmonic, due to nonuniformities in nozzle spacing.

Despite these confusing complications, a number of positive observations can be made. The following remarks apply specifically to results obtained with the 70-nozzle diaphragm.

1 At almost all speeds, vibrations at the 70th harmonic of running speed (i.e., at the nozzle passing frequency) are observed, though generally at a low stress level.

2 Over a speed range which corresponds quite closely to the predicted range of nozzle resonance vibrations in the out-of-phase modes, the stresses are high and reach a number of resonant peaks which can be associated with the predicted out-of-phase tangential modes.

3 While the experimentally measured resonant speeds in each mode fluctuate over as much as 80 rpm (about a 1.6 percent variation), the mean value for each of the out-of-phase tangential modes is between 95.1 percent and 95.5 percent of the predicted resonant speed in the 70th harmonic.

4 The observed phase relationships are fairly consistent for the first, second, and fifth mode, but agree exactly with the predicted relationships only for the first and fifth modes.

For the 126-nozzle data somewhat similar observations were made, although the observed stress-speed profiles were less consistent and therefore particular stress peaks, mode frequencies, and mode shapes could be identified with less assurance. Because of the different K-factors, the relative importance of the various modes differed, of course, from that in the 70-nozzle configuration. The relative frequency spacing between observed modes did not correspond as well to the predicted values as did that for the 70-nozzle diaphragm.

There was another significant difference between the results from the two configurations. The average ratio of measured to predicted stresses with the 70-nozzle diaphragm was more than 4 times as high as the corresponding ratio with the 126-nozzle diaphragm. In part this discrepancy may be due to the lesser reliability and completeness of the 126-nozzle stress data, but there are also three physical attributes of the blading which probably contributed. Firstly, the trailing edge thicknesses of the nozzle blades in the 70-nozzle diaphragm were found to be considerably thicker and squarer than intended, and proportionately much thicker than those in the other diaphragm. This should result in more severe wakes and hence stronger excitation. Secondly, even though the axial spacing between nozzles and rotating blades was less in the 126-nozzle configuration, it was nevertheless *proportionately* greater, when compared to the nozzle blade chord, than in the 70-nozzle configuration. Thus the wakes in the former could have decayed more before reaching the rotating blades. Thirdly, the resonant speed with 126 nozzles was of course barely half that with 70 nozzles, and the lower centrifugal loads on the blade roots, at the lower speed, could well result in higher root damping. This would account not only for the lower stresses but also for the less distinct stress peaks obtained with the 126-nozzle diaphragm.

The major emphasis of this paper will, however, be on the relationship between the measured stresses and the operating variables such as torque, mass flow, velocity ratio (i.e., ratio of wheel speed to absolute steam velocity), and derived quantities such as Mach number and Reynolds number of the nozzle exit flow. The relevant data are tabulated in Tables 3 and 4.

Since there were so many inconsistencies in the relative magnitudes of the measured stresses, an average of the stresses measured in several blades and several modes was determined for each run. These "representative" stress values, S, were then used for correlations with operating conditions. Another parameter used in these correlations has been termed "specific stress" F and represents simply the quotient of the average stress S divided by torque T. If the fractional stimulus and log decrement were

Table 3 Stresses versus operating conditions with 70 nozzles

NOMINAL COND. NO.	RUN NO.	TORQUE LB-FT T	VELOCITY RATIO v	FLOW LBS/HR G $10^3 \times$	REYNOLDS NO. Re $10^6 \times$	MACH NO. M	REDUCED FREQUENCY ω	REPR. STRESS S	S/T RATIO F	S-2.6T
1	21	930	.457	88	1.38	0.77	1.87	4540	4.87	1920
2	16	517	.524	68	1.07	0.68	2.43	3180	6.16	1770
2	20	515	.488	73	1.18	0.73	2.10	3090	6.00	1750
3	15	700	.452	71	1.15	0.79	1.82	3990	5.70	2170
4	17	930	.381	73	1.24	0.97	1.35	5760	6.20	3340
4	22	912	.403	70	1.16	0.90	1.47	5750	6.31	3380
5	9	910	.320	55	0.93	1.14	1.03	5700	6.28	3330
5	25	935	.358	60	1.03	1.03	1.23	5710	6.11	3280
6	14	235	.513	43	0.68	0.69	2.32	2240	9.53	1630
7	4	450	.428	43	0.70	0.84	1.65	3000	6.68	1830
7	13	415	.435	43	0.71	0.83	1.70	3200	7.72	2120
8	5	575	.393	45	0.74	0.91	1.42	4850	8.45	3350
9	8	1025	.280	45	0.82	1.34	0.85	2730	2.67	60
9	11	1015	.294	47	0.89	1.42	0.90	2930	2.89	290
9	12	920	.305	45	0.83	1.25	0.96	3120	3.40	720
10	3	450	.370	34	0.57	0.98	1.30	4590	10.20	3420
10	23	395	.395	33	0.56	0.92	1.43	4230	10.73	3200
11	1	420	.325	27	0.48	1.15	1.05	3810	9.05	2720

Table 4 Stresses versus operating conditions with 126 nozzles

NOMINAL COND. NO.	RUN NO.	TORQUE LB-FT T	VELOCITY RATIO v	FLOW LBS/HR G $10^3 \times$	REYNOLDS NO. Re $10^6 \times$	MACH NO. M	REDUCED FREQUENCY ω	REPR. STRESS S	S/T RATIO F	S'-1.6T
E 5	101	1220	.207	58	0.63	1.03	1.05	3310	2.71	1360
A 5	102	280	.136	11	0.15	1.91	0.62	1100	3.93	650
A 1	103	280	.234	20	0.23	0.91	1.21	740	2.64	290
B 3	113	760	.303	65	0.65	0.68	1.73	100	0.13	-1120
B 5	107	950	.232	53	0.56	0.89	1.20	2290	2.41	770
B 6	108	260	.379	39	0.39	0.53	2.43	380	1.46	-40
B 7	106	425	.306	42	0.44	0.68	1.76	310	0.73	-370
B 7	110	415	.303	39	0.41	0.68	1.73	100	0.24	-560
B 9	109	935	.189	41	0.46	1.13	0.93	3660	3.91	2160
B 9	114	940	.189	41	0.46	1.14	0.93	3280	3.49	1780
B 11	105	415	.226	24	0.27	0.94	1.16	1370	3.30	710
B 11	111	406	.209	20	0.23	1.01	1.05	1980	4.87	1330
B 12	112	1580	.222	83	0.85	0.92	1.13	3000	1.90	470

indeed fixed quantities, then the specific stress should also be a constant independent of operating conditions.

Tables 3 and 4 show that this is not so. The specific stresses (stress/torque ratios) with the 70-nozzle diaphragm ranged from about 2.7 to about 10.7. With the 126-nozzle diaphragm the specific stresses ranged from virtually 0 to almost 5. (Direct comparison between the S values for the two configurations should not be made, since the blade/mode combinations which contributed to the representative stress S differed between the two cases). Comparison of results for replicate runs at the same nominal conditions shows that the data are reasonably repeatable.

5 Correlations Between Stresses and Flow Parameters

Introduction. Our purpose in the following is to search for relationships between the measured stresses and the operating parameters. First we shall look at the results from a mainly empirical point of view, although even for this purpose some rational selection must be made of the parameters with which we seek to correlate the measured stresses. Later we shall try to rationalize the findings.

Considerations to be discussed later led to the choice of torque, mass flow, and velocity ratio as the primary parameters of interest, and the experimental program was designed to obtain data at various combinations of these parameters. Eleven different "nominal operating conditions" were chosen ahead of actual testing, on the basis of simplified performance calculations. These are listed in Table 2. The correlations were based, however, on the pressures, temperatures, speeds, torques and steam flows actually recorded during each run, and on the velocity ratios, Mach numbers, Reynolds numbers, and other derived parameters calculated from the primary measurements. These data are listed in Tables 3 and 4.

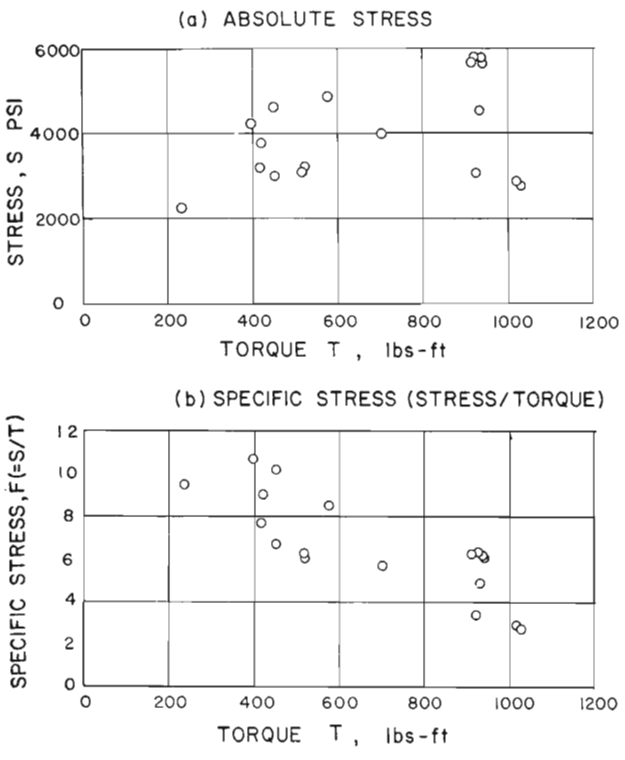

Fig. 2 Stresses versus torque (70 nozzles)

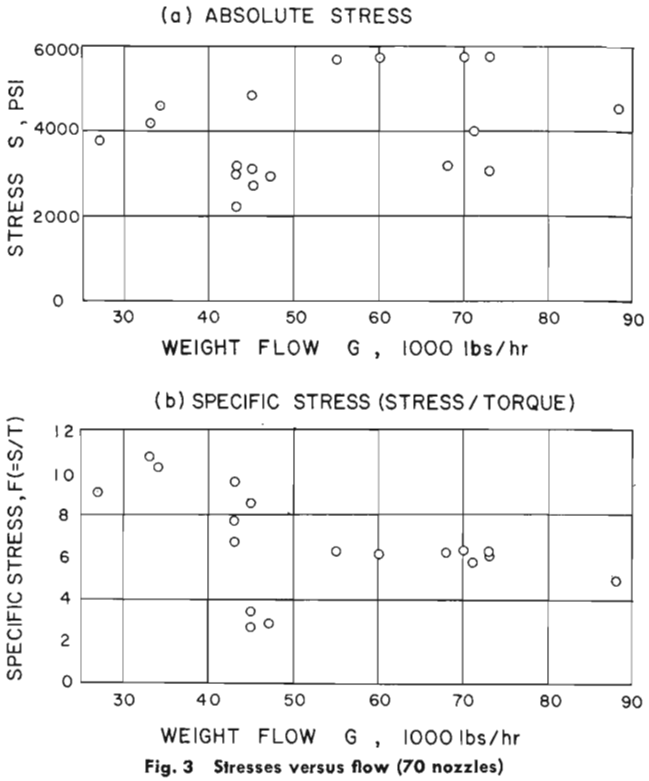

Fig. 3 Stresses versus flow (70 nozzles)

A number of approaches were utilized to seek correlations between the stresses and the operating variables, with one of the aims being to find a type of correlation which reasonably describes the results for both the 70-nozzle and the 126-nozzle configurations.

These included simple tabulations of the average data for "orthogonal" sets to deduce overall trends; graphical plotting of the data to show more detailed trends and to suggest mathematical formulations for the correlation; and finally regression analyses by computer to calculate the coefficients for the correlation equations and to check their goodness of fit. Both the representative absolute stresses and the corresponding "specific stresses" or stress/torque ratios have been examined in these correlation attempts.

Results of Correlations by Eye. Let us consider the stress and operating parameters listed in Table 3 for the 70-nozzle configuration. Figs. 2, 3, and 4 show absolute stresses (S) and specific stresses ($F = S/T$) plotted versus torque, mass flow, and velocity ratio, respectively. One can see that relative to torque, the scatter is great but there is a noticeable tendency for the stresses to increase with torque, though not nearly proportionately; consistent with this, there is a clear negative correlation between torque and specific stress. Relative to mass flow, the scatter is also great and no overall trend is obvious for absolute stresses, though specific stress seems to be negatively correlated again. The most striking correlation is found relative to velocity ratio: The scatter is less and there is a distinct trend for the absolute stresses to peak at an intermediate value of velocity ratio (0.35 to 0.40) and to drop off at lower and higher values. For specific stresses the trend is similar but less clear.

These observations suggest that a correlation of absolute stress with torque T and velocity v ratio might be a fruitful approach. If we identify the velocity ratios represented by the various points in Fig. 2(a), we find that like velocity ratios can be approximately connected by straight lines. The slope of these lines is approximately equal to 2.6. This suggests that an improved correlation might be obtained by assuming that

$$S = 2.6T + f(v) \tag{2}$$

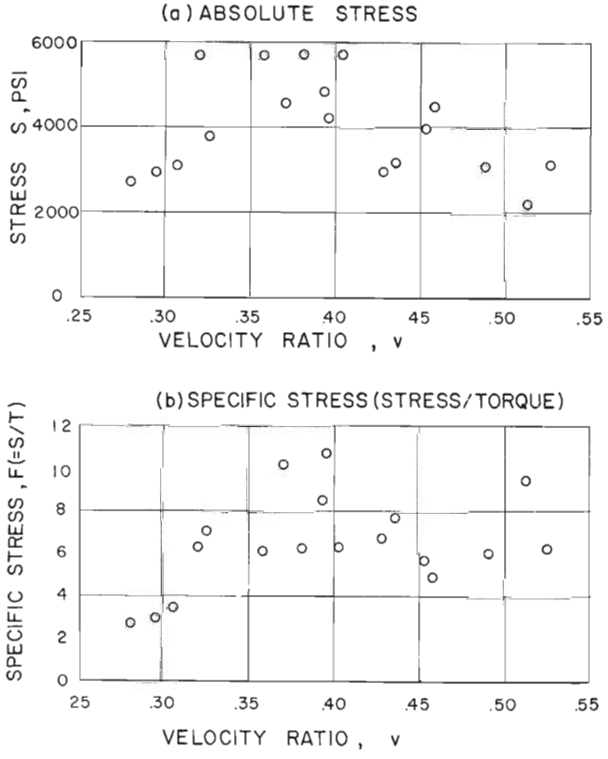

Fig. 4 Stresses versus velocity ratio (70 nozzles)

and the velocity ratio function $f(v)$ can be established by plotting $(S - 2.6T)$ versus velocity ratio. This is done in Fig. 5, and shows about as good a correlation as one could expect from data with as many inherent experimental uncertainties.

That does not mean that velocity ratio is necessarily the fundamental parameter of importance. There are a number of other "independent" parameters of possible physical significance, which are fully or strongly correlated with velocity ratio in a given configuration operated in the manner required for our tests. One of these parameters is Mach number, since the wheel

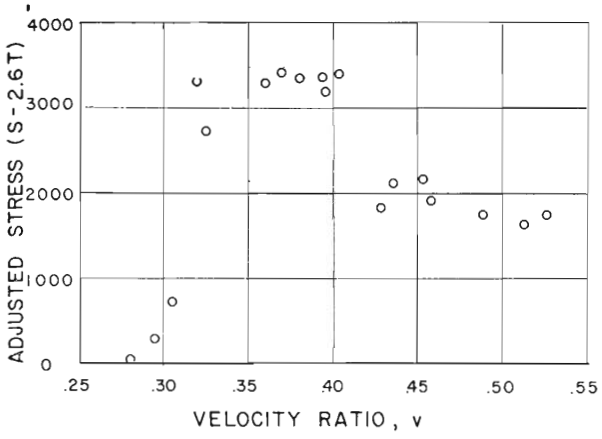

Fig. 5 Torque-adjusted stress versus velocity ratio (70 nozzles)

speed is fixed by the resonance requirement and velocity ratio can only be varied by changing the nozzle exit velocity. Thus, Mach number may equally well be the determining factor, and it is noteworthy that $M = 1$ (which corresponds to $v = 0.36$) locates the approximate peak in the curve of Fig. 5. Mach number is plotted versus velocity ratio for both of our configurations (Fig. 10).

If the foregoing correlation is to have any general validity, the 126-nozzle data should correlate in a similar fashion. These data, as has been pointed out before, are less extensive and less consistent than the 70-nozzle data. Nevertheless, we can show that they display at least the same general trends. Figs. 6 through 8 show stresses plotted versus torque, flow, and velocity ratio, similarly to Figs. 2 through 4 for the 70-nozzle data. If velocity ratios were marked for each point in Fig. 6(*a*), then one might (with a certain amount of faith!) conclude that the stress-torque relationship at constant velocity ratio is given by a straight line of slope 1.6. On this basis ($S - 1.6T$) is plotted versus velocity ratio in Fig. 9. This shows a peak at about $v = 0.18$, and what might be a minimum at about $v = 0.3$. (In fact, stresses obtained at velocity ratios of about 0.3 were either not measurable or extremely low, and the values listed for those runs in Table 4 are essentially nominal estimates.) Since the wheel speed, at resonance, is lower with 126 nozzles than with 70 nozzles, the velocity ratios at any given Mach number are correspondingly lower. Thus, in Fig. 9, $M = 1$ corresponds to $v = 0.21$, somewhat to the right of the peak in the curve which occurs at $v = 0.18$ or $M = 1.2$. The minimum at $v = 0.3$ corresponds to $M = 0.7$; this agrees well with the leveling-off or minimum point in the 70-nozzle curve, which occurs at $v = 0.51$ or also $M = 0.7$.

While the foregoing comparison suggests that Mach number may indeed be the more significant parameter than velocity ratio, since it is approximately the same for critical points in the curves both for the 70-nozzle and 126-nozzle data, there is another parameter which is likely to be important. This is the quantity which, in the literature on blade interference effects, is referred to as the "reduced frequency," ω. The greater this quantity, the greater is the number of wakes which are simultaneously interacting with the blade, and, it seems reasonable to suppose, the less will be the net fluctuating force on the blade. For our purposes, the reduced frequency will be defined as

$$\omega = \frac{\pi b}{p}\left(\frac{v}{1-v}\right)$$

where b = rotating blade chord, p = nozzle pitch, and v = velocity ratio. This is more fully explained later; see equations (9) and (12) through (15). The values of ω for our configurations are plotted versus velocity ratio in Fig. 10.

Since the reduced frequency increases with velocity ratio, it provides a plausible explanation for the descending portion of the stress curves as velocity ratio increases. Since it is proportional to the number of nozzles, it brings the 70-nozzle and 126-nozzle patterns closer together than when plotted versus velocity ratio directly.

Analytical Correlation Results. A more sophisticated correlation approach is offered by regression analysis. A "mathematical model" is proposed in the form of a prediction equation, whose coefficients are computed by a least-squares method to fit the experimental data. The results are then evaluated by various statistical tests.

Several such analyses were carried out with the aid of digital computer programs. Either specific stress F or absolute stress S, from Tables 3 and 4, was taken as the dependent parameter, and either velocity ratio v or reduced frequency ω, together with torque T, were selected as the independent parameters. The functional forms adopted for these attempts were suggested by the results of the previously described "eye-ball" correlations. The most successful of several attempts, both in terms of "goodness of fit" and of consistency between the 70- and 126-nozzle data, resulted in the following prediction equations:

70-Nozzle Data

$$S_{70} = -34{,}929 + 71{,}636\omega - 43{,}267\omega^2 + 8249.8\omega^3 + 2.848T \quad (3a)$$

$$F_{70} = -45.694 + 95{,}279\omega - 57.792\omega^2 + 10.965\omega^3 + 2115.4/T \quad (3b)$$

126-Nozzle Data

$$S_{126} = -4873.6 + 16{,}898\omega - 14{,}039\omega^2 + 3255.8\omega^3 + 1.649T \quad (3c)$$

$$F_{126} = -4.223 + 21.210\omega - 18.405\omega^2 + 4.2843\omega^3 + 360.99/T \quad (3d)$$

Equations (3*a*) and (3*c*) are of the form $S = AT + f(\omega)$, as suggested by equation (2), and equations (3*b*) and (3*d*) of the form $F = B/T + g(\omega)$. The functions AT and $f(\omega)$, for both configurations, are plotted in Fig. 11, and the functions B/T and $g(\omega)$, for both configurations, in Fig. 12. In each case, the functions of ω for the two configurations, while not identical, are similar enough (at least with respect to the values of ω at which the minimum and maximum occur) to suggest a physical significance for the parameter ω. Note, also, that the values of the torque coefficient A in equations (3*a*) and (3*c*) are reasonably close to those deduced by eye in the previous section: 2.848 as compared with 2.6, and 1.649 as compared with 1.6. Admittedly equation (3*d*) cannot be physically correct, since (Fig. 12) it would permit negative values of F for some combinations of ω and T.

The statistical significance of these correlations can be examined with the aid of Tables 5 and 6. Table 5 presents some statistics concerning the experimental data themselves: The fact that the "measurement error estimate" σ_M is considerably smaller than the standard deviation about the overall mean, σ_0, confirms that there is some systematic variation of stresses with operating conditions, and that the stresses at identical "nominal" conditions are fairly repeatable. On the other hand, σ_M also provides a lower limit to the standard deviation which can reasonably be expected of the measured values about any prediction equation; the values actually obtained are designated σ_F in Table 6.

The success of a prediction equation can be measured by the "standard error of estimate," designated σ_E in Table 6. (Each value of σ_E is somewhat higher than the corresponding value of σ_F; its definition reflects the fact that the more coefficients are computed for a prediction equation, the fewer points remain by which an independent check of its prediction ability can be made.)

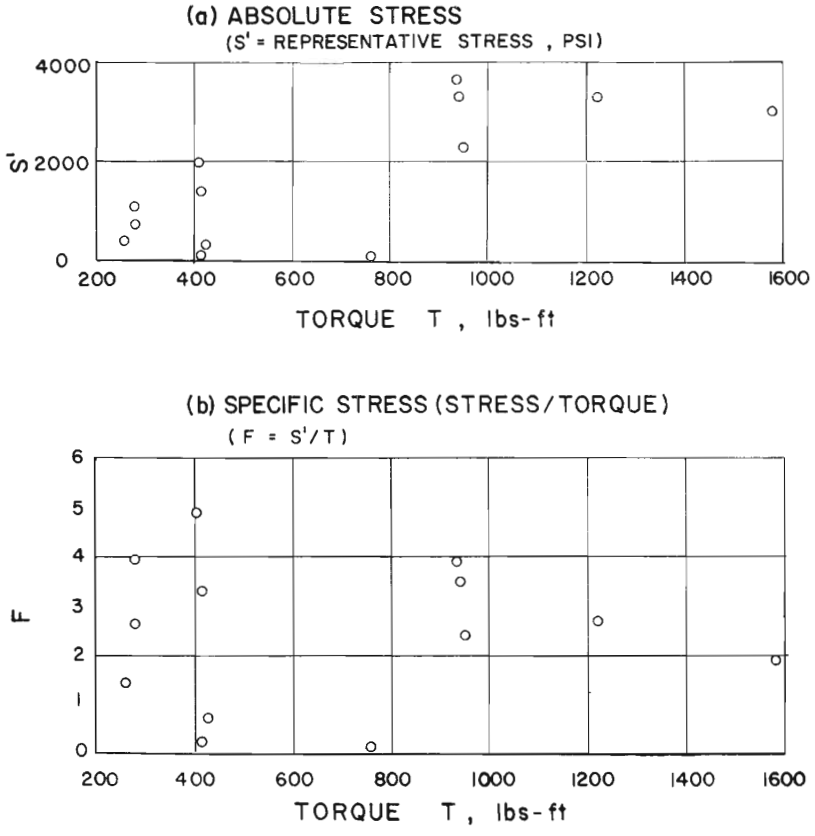

Fig. 6 Stresses versus torque (126 nozzles)

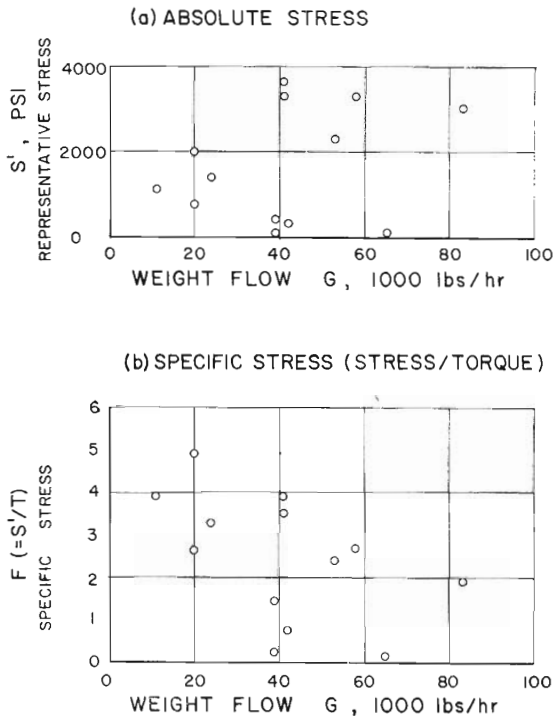

Fig. 7 Stresses versus flow (126 nozzles)

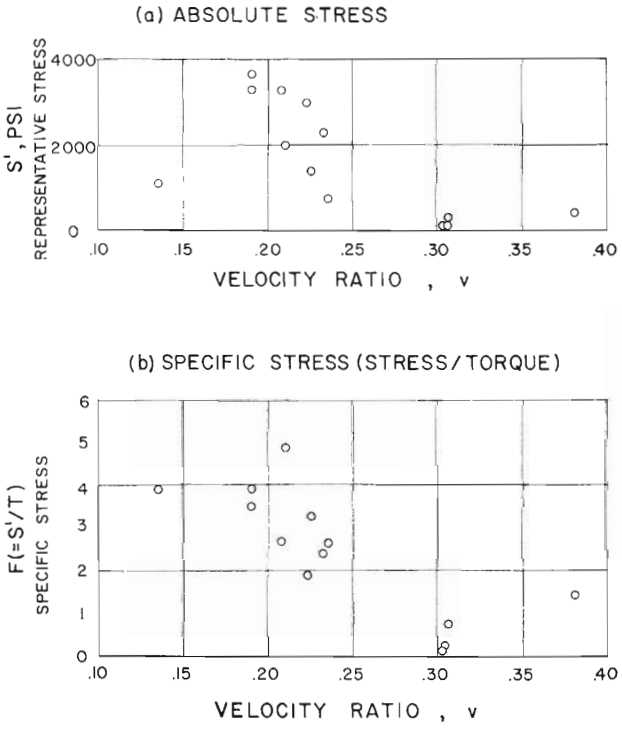

Fig. 8 Stresses versus velocity ratio (126 nozzles)

Finally, the correlation coefficient, r, is also listed in Table 6. (Its square represents the proportion of the original variance about the mean, σ_0^2, which has been accounted for by the prediction equation. Hence, $r^2\sigma_0^2 = \sigma_0^2 - \sigma_F^2$.)

A rigorous regression analysis would apply additional tests to the prediction equation and its coefficients; we can conclude from the foregoing, however, that both mathematical models give reasonable fits within the data range, but probably do not represent the true physical relationships and should not be used for any extensive extrapolation out of the data range.

For an overall comparison of the success achieved by either velocity ratio, or the related variables Mach number (M) and reduced frequency (ω), in unifying the results for the 70- and 126-nozzle configurations, the values of these parameters for the maximum and minimum points in Figs. 5 and 9, and of Fig. 11 for ω, are listed in Table 7.

It appears that M is the most successful, followed by ω, and lastly v. The discussions which follow, however, suggest that the observed variation of stresses with these parameters is likely to be, in a physical sense, a combination of the effects of several of them.

6 Discussion and Theory

Parameters Affecting Unsteady Forces on Rotating Blades. The overall geometry of the type of blading with which we are concerned, and some of the dimensional and velocity relationships which we shall later refer to, are depicted in Fig. 13.

The primary parameters which were chosen to prescribe the different operating conditions were torque, mass flow, and velocity

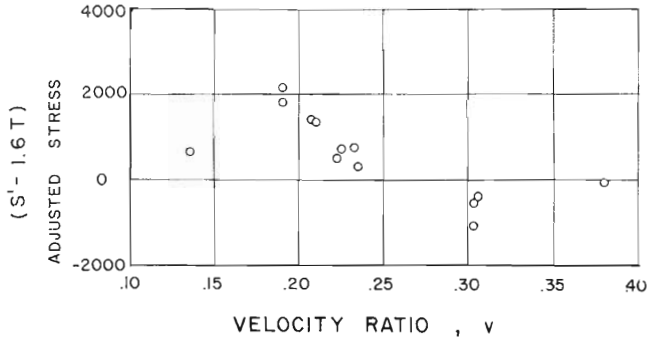

Fig. 9 Torque-adjusted stress versus velocity ratio (126 nozzles)

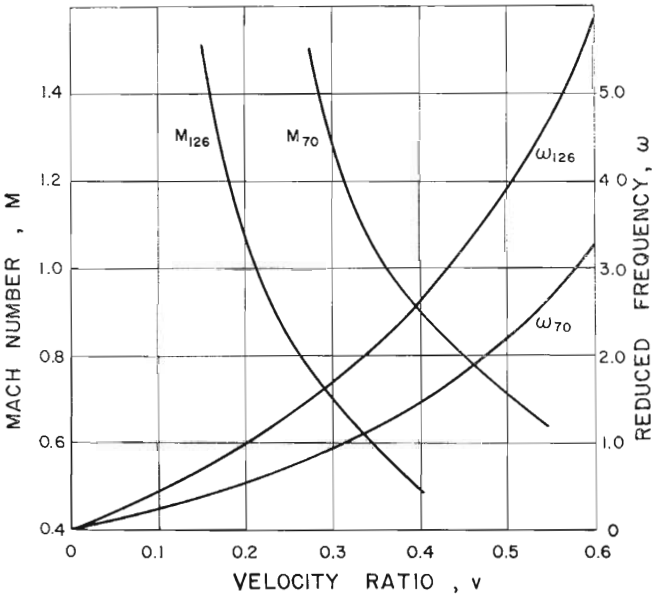

Fig. 10 Relationship between velocity ratio, Mach number and reduced frequency (for both 70- and 126-nozzle configurations)

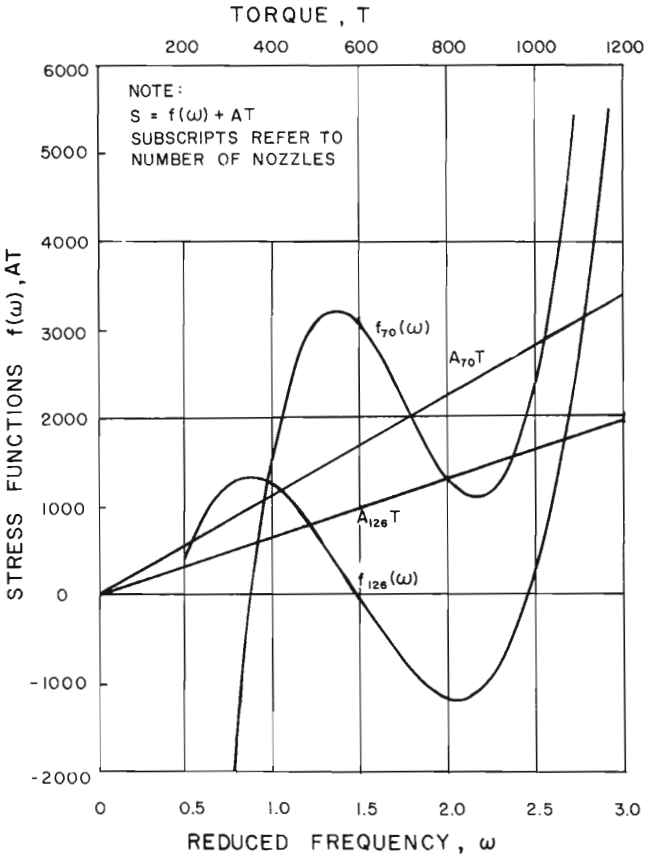

Fig. 11 Absolute stress from analytical prediction equations

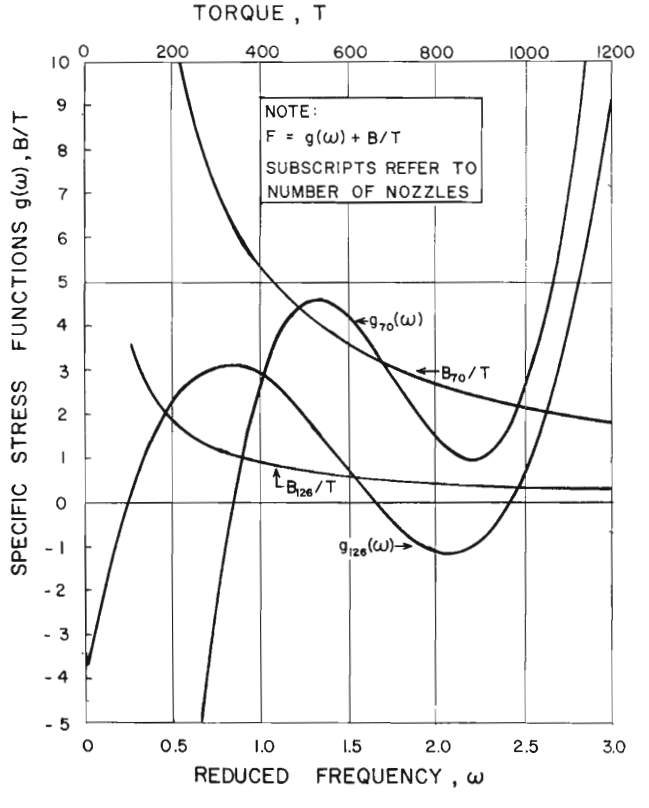

Fig. 12 Specific stress from analytical prediction equations

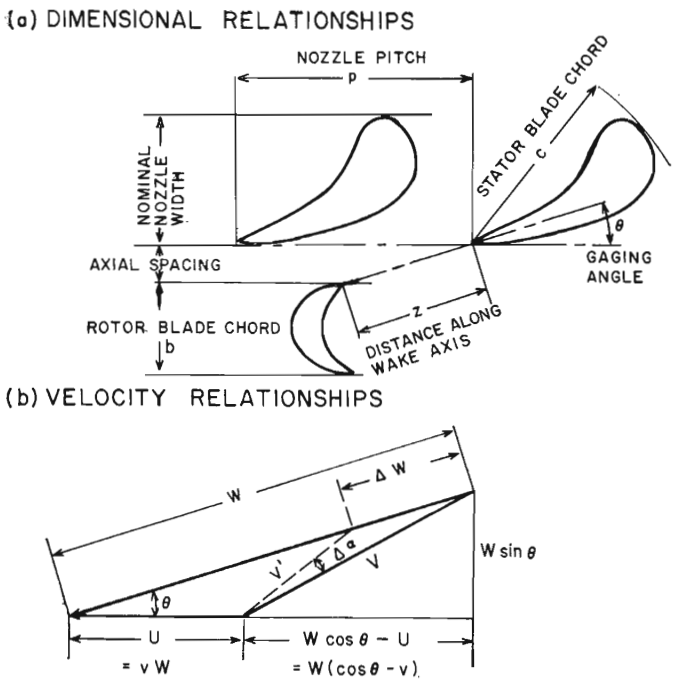

VELOCITY RATIO $v \equiv U/W$

$$\frac{U}{V} \equiv \frac{vW}{\sqrt{W^2(\cos\theta - v)^2 + W^2 \sin^2\theta}} = \frac{v}{\sqrt{1 - 2v\cos\theta + v^2}}$$

ΔW = VELOCITY DEFECT OF WAKE

V' = MINIMUM VELOCITY IN WAKE SEEN BY ROTOR BLADE

$\Delta\alpha$ = FLUCTUATION IN ANGLE OF ATTACK

Fig. 13 Geometric relationships of blading and flow

Table 6 Statistical properties of prediction equations

EQUATION NUMBER	DEPENDENT VARIABLE	STANDARD DEVIATION ABOUT EQUATION σ_F	STANDARD ERROR OF ESTIMATE σ_E	CORRELATION COEFFICIENT r
3a	S_{70}	448	512	0.919
3b	F_{70}	0.720	0.823	0.949
3c	S_{126}	397	487	0.950
3d	F_{126}	0.508	0.623	0.935

NOTE:

$$\sigma_F = \sqrt{\frac{\sum(y_M - y_P)^2}{n - 1}}$$

$$\sigma_E = \sqrt{\frac{\sum(y_M - y_P)^2}{n - k}}$$

$$r = \sqrt{1 - (\sigma_F / \sigma_0)^2}$$

WHERE

y_M = MEASURED VALUE

y_P = CORRESPONDING PREDICTED VALUE

n = NUMBER OF POINTS

k = NO. OF COEFFICIENTS IN EQUATION

Table 5 Statistical properties of experimental data from Tables 3 and 4

CONFIGURATION (NUMBER OF NOZZLES)	DEPENDENT VARIABLE	MEAN VALUE	STD. DEV'N ABOUT MEAN σ_0	MEASUREMENT ERROR ESTIMATE σ_M
70	S_{70}	4023	1135	NOT COMPUTED
70	F_{70}	6.61	2.281	0.522
126	S_{126}	1663	1277	NOT COMPUTED
126	F_{126}	2.44	1.430	0.522

NOTE:

The measurement error estimate σ_M represents a "pooled" estimate of the standard deviation of stresses obtained at the same "nominal" operating conditions. Both 70-nozzle and 126-nozzle data were pooled to compute this value.

Table 7 Consistency of correlation with velocity ratio and related parameters

CONFIGURATION	VELOCITY RATIO FROM FIGS. 5, 9	CORRESP. MACH NO.	CORRESP. REDUCED FREQUENCY	REDUCED FREQUENCY FROM FIG. 12
	v	M	ω	ω
	Values at stress maximum			
(a) 70 nozzles	0.37	0.98	1.30	1.30
(b) 126 nozzles	0.175	1.23	0.85	0.80
(c) Ratio (a)/(b)	2.11	0.80	1.53	1.62
	Values at stress minimum			
(a) 70 nozzles	0.51	0.70	2.30	2.20
(b) 126 nozzles	0.30	0.70	1.70	2.05
(c) Ratio (a)/(b)	1.70	1.00	1.35	1.08

ratio. These were not entirely independent, since pressure and temperature limitations required that if any two of these were chosen, the third was also determined.

In terms of their effect on the vibratory response of the rotating blades at nozzle resonance, the importance of torque is obvious from equation (1) and need not be further justified.

Mass flow was chosen as another test parameter because it provides an index to the Reynolds number. Although mass flow was not found to be promising as primary factor in the correlation attempts described previously, some observations concerning Reynolds number effect will be made later.

The significance of velocity ratio can be demonstrated by a very simplified discussion of the fluctuating forces acting on the rotating blades. These can be regarded as airfoils placed in a flow field which consists of a steady-state flow with a superimposed fluctuating flow. The aerodynamic force on an airfoil of unit area can be expressed as:

$$R = C\rho V^2/2 \tag{4}$$

where C is an appropriate coefficient which depends on Reynolds number and on the angle of attack, if V is steady. If we assume that V consists of a steady component V_S and a sinusoidally varying component V_P of angular frequency ν, then

$$V = V_S + V_P \sin \nu t \tag{5}$$

and, in quasi-steady form,

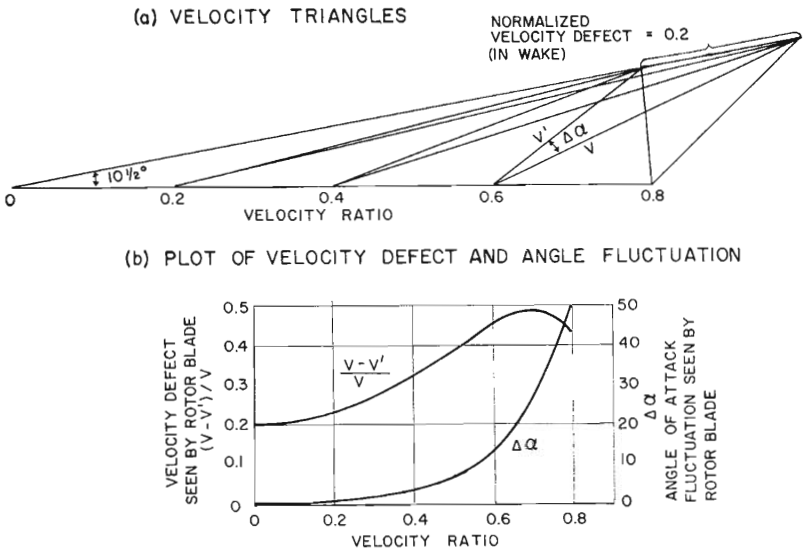

Fig. 14 Velocity fluctuations seen by rotor blade versus velocity ratio

$$R = \frac{C\rho}{2}\,(V_S^2 + 2V_S V_P \sin \nu t + V_P^2 \sin^2 \nu t) \qquad (6)$$

The amplitude R_P of the fluctuating force component of frequency ν can be expressed as

$$R_P = C_P \rho V_S V_P \qquad (7)$$

Since, in general, the angle of attack will be fluctuating as well as the flow velocity, and because of other nonsteady effects, the effective coefficient of this term, written as C_P, will differ from the coefficient for the steady component C_S. Dividing the pulsating force by the steady force represents, by definition, the fractional stimulus. Thus

$$\psi \equiv \frac{R_P}{R_S} = \frac{2C_P}{C_S}\,\frac{V_P}{V_S} \qquad (8)$$

Now V_P/V_S is the nondimensional fluctuating velocity *as seen by the blade*, and this depends not only on the fluctuations in the absolute steam velocity, which one would measure as one slowly traverses across the wakes issuing from the nozzles, but depends also on the velocity ratio. This is evident from Fig. 13(*b*) and is further illustrated in Fig. 14, from which one can clearly see that, with the absolute velocities remaining constant, the blade sees both a greater relative fluctuation of the approach velocity, and a greater fluctuation in the angle of attack, as the velocity ratio increases. The fluctuation in the angle of attack will affect the ratio of unsteady to steady aerodynamic force coefficients, C_P/C_S, so that this term also becomes velocity ratio dependent. These quasi-steady arguments should suffice to show why velocity ratio in itself is significant and was therefore chosen as one of the primary variables in the experimental design and data correlation.

It turns out, however, that there is another, more indirect, way in which velocity ratio exerts an influence on C_P/C_S. Intuitively one may argue that the greater the number of wakes which simultaneously interact with a given blade, the more will the individual wake effects overlap, and the less will be the net effective "kick" which each new wake imparts to the blade. In other words, the effective aerodynamic force coefficient for the unsteady flow component should be a function of the number of wakes which are simultaneously acting on a given blade, or, equivalently, of the ratio of the time taken for a wake to pass along a blade to the time taken for the blade to progress from one wake to the next. The exact determination of this is difficult since we do not know the exact velocity in the wake, but an index to this quantity would be given by using, as the numerator in the ratio, the time represented by the passage past the blade of a

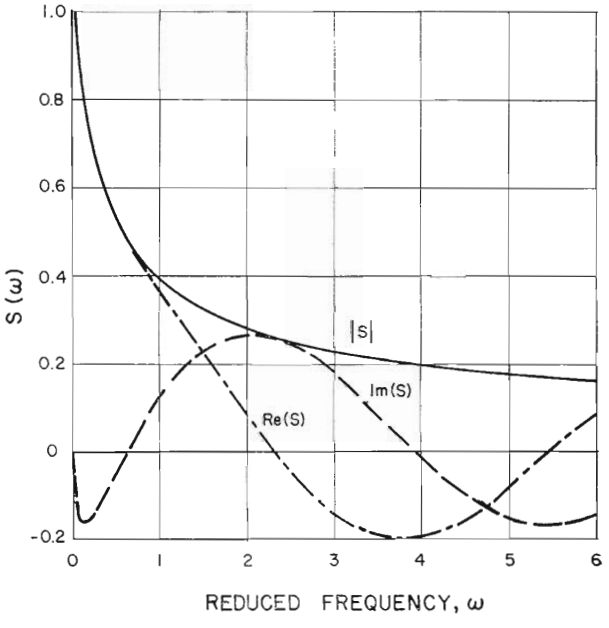

Fig. 15 "Sears function" $S(\omega)$. (Plotted from: Yeh, H., *Journal of Aeronautical Sciences*, Vol. 24, 1957, p. 546; and Kemp, N. H., *Journal of Aeronautical Sciences*, Vol. 19, 1952, p. 713)

fluid particle moving at the nominal or mean approach velocity relative to the blade. It turns out that this parameter is identical (except for a constant) to the quantity which is referred to as the "reduced frequency" in the literature on wing flutter, unsteady airfoil theory, and blade interference effects. Kemp and Sears [3, 4] define reduced frequency as

$$\omega = \nu b/2V \qquad (9)$$

where

- $\nu = 2\pi U/p$ = circular frequency (nozzle passing frequency) in radians/sec
- U = peripheral speed of rotor blades
- p = stator blade or nozzle pitch
- b = rotor blade chord
- V = speed of mean flow relative to rotor blade

This "reduced frequency" becomes an important parameter in calculating the magnitude and phase of the unsteady lift and moment on the rotating blades. The analyses of references [3] and [4] are built up from theory for an isolated thin airfoil subjected to a sinusoidally varying upwash V_U superimposed on a

steady flow velocity V_S. For that case, the sinusoidally varying lift $L(t)$, of frequency ν, is given by

$$L(t) = \pi\rho V_S V_U S(\omega) e^{i\nu t} \tag{10}$$

All terms herein have been previously defined except for the complex function $S(\omega)$ which represents the influence of reduced frequency ω. This is the so-called Sears function, and is defined as:

$$S(\omega) = \{i\omega[K_0(i\omega) + K_1(i\omega)]\}^{-1} \tag{11}$$

where K_0 and K_1 are modified Bessel functions of the second kind. This is plotted in Fig. 15.

Comparison of equations (10) and (7) will show that the magnitude of $S(\omega)$ is loosely analogous to what we have termed C_P, though not exactly because V_P represents not merely an up-wash velocity V_U but any sinusoidal fluctuation of V.[3] The writer made some attempts to apply Kemp's and Sears' analysis to the blading with which we are concerned here, but it soon became apparent that the geometries were so different that some of their definitions became meaningless for our case and many of their simplifying assumptions certainly do not apply. Nevertheless, the reduced frequency can be expected to be important in our case too. Combining equation (9) with the definition of ν, we can obtain

$$\omega = \pi \frac{b}{p} \frac{U}{V} \tag{12}$$

From Fig. 13(b) it can be seen that the ratio U/V depends on gaging angle θ and on velocity ratio v. The exact expression is

$$\frac{U}{V} = \frac{v}{[1 - 2v\cos\theta + v^2]^{1/2}} \tag{13}$$

but when θ is small enough for $\cos\theta \simeq 1.0$, and v is relatively small, it can be approximated as

$$\frac{U}{V} \simeq \frac{v}{1 - v} \tag{14}$$

Hence for our purposes the reduced frequency will be defined as

$$\omega = \frac{\pi b}{p}\left(\frac{v}{1 - v}\right) \tag{15}$$

Thus we have a parameter which, for a given geometry, is fully correlated with velocity ratio so that its effects cannot be distinguished from those of other effects or parameters which are dependent on or correlated with velocity ratio.

Moreover, as we have discussed earlier, the Mach number of the nozzle exit flow is also closely determined by velocity ratio. Mach number, if high enough to make the flow compressible, can be expected to influence the character of the flow around the nozzle blades and, therefore, of the wakes.

One approach for distinguishing between velocity ratio, reduced frequency, and Mach number effects in the experimental results, lies in comparing the 70-nozzle results with the 126-nozzle results, since these parameters bear different relations to one another in the two configurations. This was done in Table 7. Another approach is to compare the observed trends with the probable physical consequences of varying each of these parameters; this approach will be used in the following.

Stress Dependence on Torque and Related Parameters. The correlation attempts described previously resulted in expressing either the actual stress, or the stress/torque ratio, as the sum of a torque function and a velocity ratio function. In the former case, the torque function was a straight line of positive slope; in the latter case the torque function was proportional to the reciprocal of torque.

Both cases, of course, represent the same data and reflect the interesting fact that, even for a fixed velocity ratio, the vibratory stresses increase less than proportionately with the torque or with the steady-state tangential steam force. Two possible explanations or contributory reasons follow:

The first is the well-known fact that the material damping coefficient generally increases with stress level. If this also applied to the overall damping of blade groups (in which other damping mechanisms act as well), then the vibratory response of a blade group would be less than proportional to torque, even though the exciting forces were proportional to it. Supporting evidence for this supposition is given by Kolb [8]. His turbine test results also exhibit a decreasing ratio of vibratory stress to load as the load (steam flow) increases, and he shows experimental resonance curves of actual blades, for which the calculated log decrements increased significantly with peak stress amplitude. Similar results, from static vibration tests of simulated blades and shrouded blade groups, have been shown, for instance, by Pisarenko [9].

The second possible contributory reason does involve the supposition that, at least in our particular tests, the fractional stimulus decreased with increasing torque because of a Reynolds number effect. To increase the torque while maintaining a constant velocity ratio, the overall density level and mass flow, and hence Reynolds number, must be increased. Specific stresses (for the 70-nozzle configuration) have been plotted versus Reynolds number in Fig. 16(a). The fractional stimulus may be

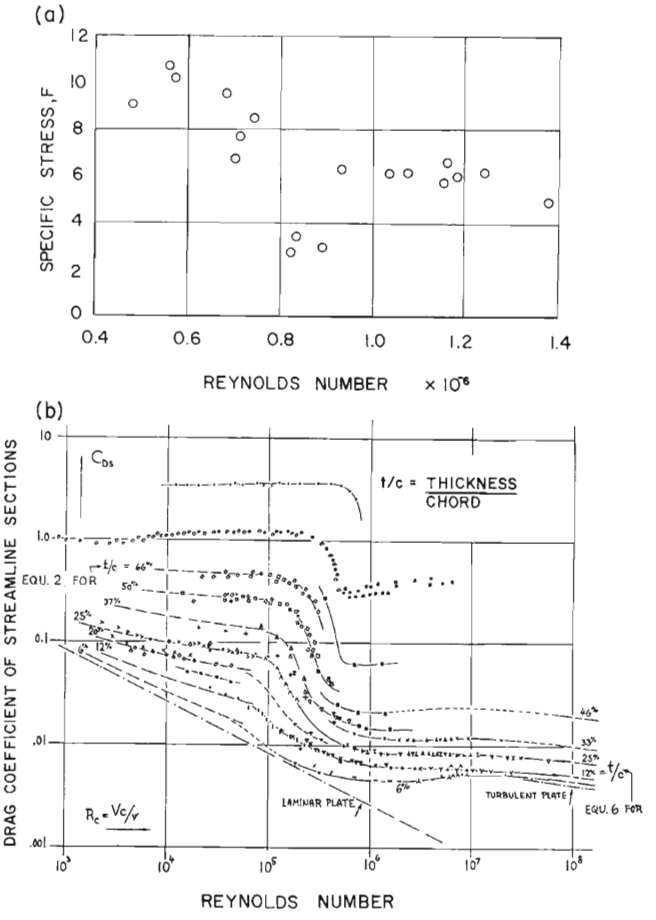

Fig. 16 Reynolds number effects:
(a) specific stress versus Reynolds number in 70-nozzle configuration
(b) drag coefficient of streamline sections versus Reynolds number (adapted from Fig. 2, Chapter 6 of reference [10], with author's permission)

[3] An extension of the Kemp-Sears method, which adds the effect of chord-wise gusts to the up-wash or transverse gusts, was recently given by Horlock [16].

related to Reynolds number through the stator drag coefficient.

Kemp and Sears [4] have predicted that the unsteady forces of the moving blades, due to the viscous wakes from the stator blades, will be proportional (or nearly so) to the profile drag coefficient of the stator blades, which in turn depends on Reynolds number. Fig. 16(*b*) shows plots of drag coefficients versus Reynolds number for streamline sections, reproduced from Hoerner [10]. It is quite striking that the range of our experimental Reynolds numbers, from 0.4×10^6 to 1.4×10^6, falls almost exactly into the transition region between laminar and turbulent flow, in which the drag coefficients vary strongly with Reynolds number. Moreover, the variation of specific stress with Reynolds number in Fig. 16(*a*) bears a strong resemblance to the variation of drag coefficient with Reynolds number in Fig. 16(*b*). In short, the predominant characteristic of a decrease in drag coefficient (and hence in fractional stimulus) with increasing Reynolds number is consistent with, and may explain, the observed decrease in specific stress with increasing torque and, hence, Reynolds number.

For the 126-nozzle data the overall trend is also a decreasing one with increasing Reynolds number, but there is no obvious leveling-off as in Fig. 16(*a*). This seems consistent with the fact that the range of Reynolds numbers is lower, from 0.15×10^6 to 0.85×10^6, and thus falls more nearly into the region of strongly decreasing drag coefficients in Fig. 16(*b*).

Before accepting this agreement at face value, it would be well to note some reservations. Firstly, our nozzles are not uncambered shapes operating at zero lift, as are those which provided the data for Fig. 16(*b*). Secondly, our Reynolds number is based on nozzle exit velocity and density rather than free-stream values as for Fig. 16(*b*). Thirdly, the major contribution to the unsteady forces in our type of turbine stage has been supposed [11] to come from circulation effects rather than from viscous wake effects, and the stator drag coefficient does not play a role in that contribution. Without a more thorough analysis it cannot definitely be said whether the aforementioned similarities represent a real cause-and-effect or are merely fortuitous.

Stress Dependence on Velocity Ratio and Related Parameters. The relationship between stresses and velocity ratio deduced earlier from our data depicts the stresses as at first increasing steeply with velocity ratio, reaching a peak or possibly a plateau, then decreasing to what might be constant value at high velocity ratios, or possibly a minimum followed by another increase. Figs. 5, 9, 11, and 12 do suggest a final increase, though the data do not extend to sufficiently high velocity ratios to establish this with authority.

First let us consider the velocity ratio effect mentioned earlier in this section, namely, that for a given peripheral variation in the absolute steam velocities issuing from the nozzles, the variations both in velocity and angle *as seen by the rotating blades* increase with velocity ratio.

Experimental data on wakes in cascades (albeit at low Mach numbers) have been given, for instance, by Mori [11]. From these it appears that the ratio of minimum velocity in the wake to the main stream velocity outside the wake is about 0.7 to 0.9. Fig. 14 suggests that with such ratios the fluctuations in the steam velocity and angle relative to the blade will become drastic only at high velocity ratios, say above $v = 0.5$. It therefore seems unlikely that this is the proper explanation for the initial steep rise in stresses with the velocity ratio, though it could well explain the second rising portion of the curve, if there is one, at high velocity ratios.

This is not to say that the effect is negligible at low velocity ratios. To examine it more precisely, the nondimensional velocity fluctuation and the angle of attack fluctuation, as seen by the blade, are plotted versus velocity ratio in Fig. 14(*b*). (These curves assume that the maximum velocity defect in the wake, $\Delta W/W$, is 0.2, and that the absolute velocities W and $W - \Delta W$ are both at the same angle, namely, the gaging angle which is 10.5 deg in our case. This may not always be a good assumption.) This figure shows that in the general range of our tests, between $v = 0.2$ and 0.5, the velocity fluctuation seen by the blade increases almost linearly by about 65 percent. Thus the overall trend of the stress versus velocity ratio pattern ought surely to be influenced by this effect.

Let us return to consideration of the steeply rising portion of the stress-velocity ratio pattern at low velocity ratios. As was noted earlier, the peak or plateau which terminates this portion did not occur at the same velocity ratio in the 70-nozzle and 126-nozzle configurations but did occur at similar Mach numbers and, more significantly, occurred in the vicinity of Mach 1. It seems possible, therefore, that this portion of the curve represents, in fact, a decrease in the stimulus as the velocity ratio becomes very small and the flow becomes supersonic. In this case, some pattern of expansion waves and shock waves will be established downstream of the nozzles and the character of the flow fluctuations seen by the blade could undoubtedly be greatly altered from that measured in low-speed tests (as in reference [11]) or that predicted from viscous wake theory (reference [4]) or potential flow theory (references [3] and [12]). Whether, in fact, the effect would be to reduce the peripheral nonuniformity in velocity (or at least the component of it which is periodic with the nozzle spacing), the writer cannot say and can only recommend that this topic be further pursued.

Finally, we have to explain the intermediate portion of the stress-velocity ratio curve, where the stress decreases with increasing velocity ratio. This is counter to the effect expected from the velocity ratio itself, as shown earlier. The Mach number range is the high subsonic and transonic range, about 0.7 to 1.1. Whether, in this range, increasing compressibility effects could lead to increased effective wake strengths is, once again, a question which the writer cannot answer. It is certain, however, that the variation of stresses in this range is consistent with their presumed dependence on the reduced frequency (ω).

As was shown earlier, see equation (10), the fluctuating lift force can be assumed proportional to the Sears function $S(\omega)$, other things being equal. From Fig. 15 one can see that the absolute value of $S(\omega)$ diminishes sharply with increasing ω at first, tending to level off above approximately $\omega = 2$. While the function $S(\omega)$ may not be exactly applicable to an impulse blade with its great curvature, the minimum in the specific stresses occurred at about $\omega = 2.2$ and $\omega = 2.0$, respectively, for the 70- and 126-nozzle configurations (see Fig. 12), which is quite consistent with the hypothesis that the negative-slope portion of the stress-velocity ratio pattern is related to the reduced frequency effect.

In summary, if the suppositions described above are correct, then (in the subsonic range) two conflicting trends occur as velocity ratio is increased: The increasing reduced frequency tends to reduce the excitation experienced by the blades while the velocity ratio effect itself tends to increase the excitation. As a result a minimum occurs at some intermediate value. It would seem desirable to operate at reduced frequencies greater than say 1.5 and at velocity ratios less than say 0.55.

If this is true, then the fact that the minimum stress occurred at about Mach 0.7 in both configurations would seem to be fortuitous. There is no question, however, but that further study of the influence of Mach number would be desirable, particularly to determine whether the low stresses found at supersonic Mach numbers can be explained thereby.

7 Effects of Spacing and Size

Experimental Findings With Variable Axial Spacing. Since the nonuniformities in the flow issuing from the nozzles can be expected to die out in distance, it seems reasonable to suppose that increasing the axial spacing between nozzle trailing edges and blade-leading edges might reduce the vibratory stresses. In order to test this hypothesis, provision had been made for convenient axial adjustment of the spindle in the test turbine facility. With

the 70-nozzle diaphragm, minimum or the "normal" axial spacing between the nozzles and blades was about 0.170 in. and maximum about 0.295 in.

Comparisons between stresses at minimum and maximum spacing are presented in Fig. 17. The quantity F is again the stress divided by the torque, or specific stress. The quantity F/F_N is the ratio of F to that at normal spacing. Fig. 17 shows that the greater the velocity ratio is, the greater is the reduction of specific stress effected by increasing the axial spacing to the maximum amount. It is interesting that at low-velocity ratios F/F_N is actually greater than unity, and that the intercept with unity occurs at a velocity ratio of about 0.32, corresponding to a Mach number of about 1.15.

The outlying points in Fig. 17 all derive from those runs in which the steam conditions were changed to maintain constant torque as the spacing was increased. In retrospect this was not a good procedure, since the stresses can be more sensitive to changes in velocity ratio than changes in torque. If the effects of velocity ratio changes were accounted for, these points would move towards the curve shown.

The foregoing compares the stresses obtained at the two extremes of axial spacing. It is also important to find out how the stresses vary between these extremes. Values of F/F_N are plotted directly versus axial spacing in Fig. 18, and the surprising thing about these curves is that the variation of F with spacing is by no means a linear one or even nearly so. All curves show a distinct hump and reach a maximum value of F at an intermediate spacing. Here, again, some effect of changing velocity ratio is included.

It is worth noting that there are both theoretical and experimental findings elsewhere in which interaction forces do not decrease monotonically with increasing axial spacing, but rather exhibit minima and maxima: An application of the Kemp-Sears analysis to calculate the unsteady forces on pump-jet blades showed that a maximum could occur at a finite axial clearance [13]. This probably occurs because the phase relationships between the various components of the total flow nonuniformity (i.e., circulation effects and viscous wake effects) vary with distance downstream of the stationary blades, reinforcing or canceling each other as the case may be. This is consistent with an experimental curve presented by Lewis [14], in which the unsteady force on a ship's rudder (due to passage of the propeller blades ahead of it) fluctuates with axial clearance, going through a minimum and later a maximum as the clearance is increased.

These findings apply to the 70-nozzle configuration. In some tests with the 126-nozzle diaphragm, the spacing was varied in steps between 0.137 (the normal value) and 0.230 inch. In these tests, the representative specific stress did not vary significantly with changes in the spacing. The nondimensional spacing with 126 nozzles was still greater than that with 70 nozzles, which may account for this difference in behavior. This will be further discussed below.

To conclude the present discussion, it does not seem justifiable to suppose that increasing the axial clearance between stationary and rotating blades will necessarily reduce nozzle resonance stresses, although if spacing is sufficiently increased the excitation must eventually diminish.

Discussion of Size and Spacing Effects. The influence of the overall or relative sizes of the stationary and rotating blades is obviously intertwined with the influence of axial spacing. Let us attempt to explain some of the differences between the 70 nozzle results and 126 nozzle results.

The results presented earlier have shown that the excitation, as represented by the specific stresses, of the rotating blades was considerably lower with the 126-nozzle diaphragm than with the 70-nozzle diaphragm. It also appeared that the excitation varied less with axial spacing in the former case than in the latter. Now it is important to realize that the stationary blades in the 126-nozzle diaphragm were smaller than those in the 70-nozzle

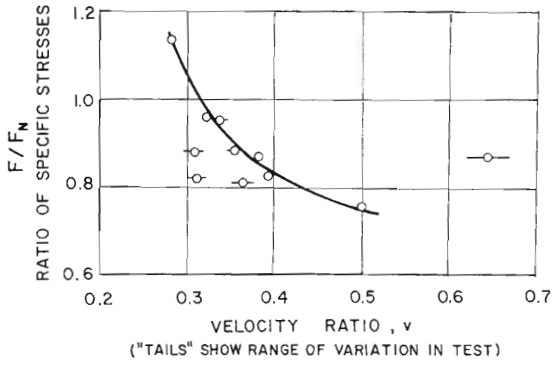

Fig. 17 Ratio of specific stresses at maximum and normal axial spacing versus velocity ratio

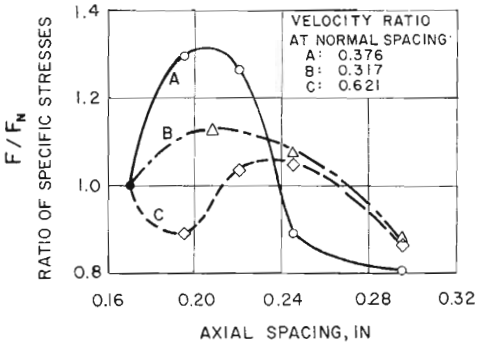

Fig. 18 Variation of specific stresses with axial spacing

diaphragm, so that the solidity (chord/pitch ratio) for the stator blading was very nearly the same for both configurations. The theoretical results of references [3] and [4] both predict that the unsteady lift coefficient for the rotor blades is a function, among other things, of the stator blading solidity and of the nondimensional spacing (referred to the stator chord) between the rotor and stator blades, but not of the absolute size of the stator directly. Thus the specific stresses should have been about the same in our two configurations if similarity had prevailed in all other matters.

One of the matters in which similarity did not prevail was the trailing edge thickness. The influence of trailing edge thickness on the unsteady circulation effects is not known to the writer, but an estimate can be made of its influence on the viscous wake effect, since this is dependent on the stator drag coefficient [4]. Some data on drag coefficients of airfoils with cut-off trailing edges are given by Hoerner [10]. From Figs. 40 and 41 in his Chapter III, one would surmise that the difference in trailing edge thickness/chord ratios (1 percent for the 126 nozzles and 2 percent for the 70 nozzles) would be responsible for only a 25 percent to 30 percent increase in drag coefficient, which does not by itself seem sufficient to explain the stress difference found experimentally, which amounted to a factor of about 2.5.

Another of the matters in which similarity did not prevail is the ratio of rotor blade chord to stator blade chord, and the ratio of stator-rotor spacing to stator chord. The first-mentioned ratio does not explicitly appear in the Kemp-Sears results but can indirectly affect the second-mentioned ratio, which will be apparent from the following: Kemp and Sears [4] consider the rotor blade as an isolated airfoil subjected to a periodic upwash whose magnitude remains constant as it passes by the blade. This upwash is determined from nominal values of the wake properties calculated at an essentially arbitrary point along the rotor blade chord, such as the quarterchord point. This point then defines the effective stator-rotor spacing, which consequently depends on the rotor blade chord length.

Admittedly, it seems questionable whether such a procedure would be valid for the high-solidity, high-turning rotor blade

Table 8 Nondimensional stator-rotor spacing for test configurations

CONFIGURATION (number of nozzle blades)	AXIAL SPACING TO LEADING EDGE*	z/c FOR LEADING EDGE	z/c FOR 1/4 CHORD
70	(Min.) 0.168 in.	0.53	1.15
	(Max.) 0.295 in.	0.94	1.55
126	(Min.) 0.136 in.	0.75	1.84
	(Max.) 0.230 in.	1.27	2.36

NOTE: * Axial spacing to 1/4 chord point is 0.197 inch greater than axial spacing to leading edge.

c = stator (nozzle) blade chord

z = downstream distance from stator blade trailing edge, in direction of steam flow

cascade of an impulse turbine stage. Theoretical analysis of this matter is complicated because once the fluid enters the rotating blade row it is chopped up into separate channels and the undisturbed flow field picture is no longer correct. This is related to what Lefcort [7] calls the "wake distortion effect."

It may nevertheless be instructive to calculate the nondimensional spacing for our test configurations. Table 8 shows that, despite an attempt to improve geometric similarity by running the rotor blades closer to the 126-nozzle diaphragm than to the 70-nozzle diaphragm, the normal nondimensional spacing was still considerably greater for the 126-nozzle configuration than for the 70-nozzle configuration. (Specifically, 42 percent greater if based on leading edge, and 60 percent greater if based on quarterchord point.) Moreover, when one compares the ranges over which the nondimensional spacing was varied, these overlap only barely when based on the leading edge point and not at all when based on the quarterchord point.

This may well contribute to the lower stresses found with the 126-nozzle diaphragm. It surely helps to explain why the variation of stresses with axial spacing with the 126-nozzle diaphragm differed from the corresponding results with the 70-nozzle diaphragm, and, perhaps, why such variation was negligible in the former case.

One final point may be of interest in relation to spacing effectss The wakes from the stator blades, as described by Kemp and Sears [4] or by Mori [11], can be represented by a characteristic "velocity defect" and a characteristic wake width. With increasing downstream distance, the velocity defect decreases and the wake width increases. The "pulse strength" associated with the wake can be represented by the product of the velocity defect and the wake width. This product will decrease with increasing distance.

However, in evaluating the effect on the excitation of the rotating blades, it is the picture seen by the rotating blades that counts and the velocity triangulation or velocity ratio effect must once more be considered. The reduction of the absolute velocity defect will result not only in a reduction of the relative velocity perturbation, but also in a reduction of the angle of attack perturbation, as seen by the rotating blade. Thus the unsteady force on the rotating blades will have a stronger dependence on the wake perturbation velocity than on wake thickness, and the blade excitation should diminish more rapidly with distance than the absolute wake pulse strength suggests. The foregoing argument should become more forceful as the velocity ratio, and consequently the angular perturbation, increases (see Fig. 14). This, perhaps, may help to explain why increasing the axial spacing seemed to reduce stresses more effectively at higher velocity ratios, as suggested by Fig. 17.

8 Summary

Vibratory stresses due to nozzle resonance have been measured in a single Rateau stage test turbine under various operating conditions. The results have been compared with predictions made in accordance with a standard calculation method, and have been discussed in the light of available theories and hypotheses.

The rotating blades were shrouded into six-blade groups, and the particular modes of vibration investigated were the five out-of-phase tangential modes, which occur in a fairly narrow frequency band. Tests were run with two alternative nozzle diaphragms, one with 70 nozzles and one with 126 nozzles. The rotational speed required for nozzle resonance was, of course, different in the two configurations. Tests were run at a variety of combinations of torque, mass flow, and velocity ratio to investigate the dependence of the stresses on these and related variables.

It was found that the observed resonant frequencies were approximately 95 percent of the predicted values. The relative stress magnitudes in the different blades differed considerably from the predictions and never exhibited the symmetry which the theory predicts. This may be due to the simultaneous excitation of several modes.

The main emphasis of this paper is on the dependence of the vibratory stresses on various operating variables. The ratios of "representative stresses" to turbine torque, under different operating or flow conditions, varied from about 3 to 10 with the 70-nozzle diaphragm, and from near 0 to about 5 for the 126-nozzle diaphragm.

The experimental results reported here suggest that, at constant velocity ratio, the stresses increase with torque but not proportionately, so that the stress/torque ratio decreases with increasing torque. Two factors may contribute to this: One is a Reynolds number effect; the range of Reynolds numbers in these tests coincided with the transition region between laminar and turbulent flow of streamline shapes, and may result in a reduction of the relative wake severity from the nozzle blades as the Reynolds number increases (which it must do when torque is increased at a constant velocity ratio). This means that the "fractional stimulus" decreases as the torque increases. The other factor is that the damping coefficient of the blades increases with the stress level, so that the resultant vibratory stress is not proportional to the exciting force.

The experimental results further suggest that when the velocity ratio is increased while the torque is maintained constant, the stresses first increase steeply to a peak or plateau, then diminish more gradually to a lower value or minimum and may finally increase once more, perhaps quite steeply, above $v = 0.5$.

Qualitative theoretical considerations lead to the hypotheses that the final increase is due directly to a geometrical velocity ratio effect, that the intermediate (negative slope) portion is due to a "reduced frequency" effect, and that the initial steep positive slope may be a Mach number effect. The "reduced frequency" may be considered as a measure of the number of wakes in simultaneous engagement with a rotating blade; it is proportional to the ratio of blade width to nozzle pitch and is also a function of velocity ratio. The greater this parameter is, the smaller may be presumed to be the net "kick" imparted to the blade by each wake it encounters, since the effects of the separate wakes will more and more overlap. This parameter has been found to be important in related studies found in the literature.

In some of the tests the axial spacing between stator and rotor blades was varied, and it was found that when this was done the stresses increased at first and then tended to decrease as the spacing was further increased. The ratio of stresses at maximum spacing to those at minimum (normal) spacing seem to show a dependence on velocity ratio. This stress ratio diminishes as velocity ratio increases, and at low velocity ratios it may exceed unity.

The great difference between stresses obtained with the 70-nozzle diaphragm and those obtained with the 126-nozzle dia-

phragm at corresponding torques is thought to be attributable to the following:

1 The nozzle blade trailing edges in the 70-nozzle diaphragm were proportionately considerably thicker than those in the 126-nozzle diaphragm, resulting in more severe wakes.

2 The nondimensional axial spacing between stator and rotor was greater in the 126-nozzle diaphragm than in the 70-nozzle diaphragm, allowing the wakes to dissipate more.

3 The lower centrifugal stresses at resonant speed with the 126-nozzle diaphragm may result in higher blade root damping, thus decreasing resonant response.

In the discussions concerning the "reduced frequency" effect, and the axial spacing effect, qualitative use has been made of the theoretical findings of Kemp and Sears; it must be emphasized, however, that the geometry of steam-turbine impulse blading is very different from the idealized model assumed by Kemp and Sears, and their results cannot be applied quantitatively. There is a great need for both theory and additional experimental data applicable to impulse stages with high turning. This applies both to the nature of the "wakes" or flow nonuniformities downstream of the nozzles, particularly at high Mach numbers, and to the unsteady forces experienced by strongly cambered blades. In this study, the forces could only be deduced from the resonant vibratory response which of course involves many other factors as well.

Acknowledgments

The writer is indebted to many individuals who contributed to this study. The experimental phase of the program depended strongly upon data acquisition and processing techniques devised by R. L. Osborne and D. W. Darkow. H. Ginsburg of the Westinghouse Research Laboratories provided important advice and assistance in the statistical design of experiment and data analysis. Finally, A. J. Partington, F. C. Bertolet, and others contributed valuable discussions relating to the physical interpretation of the results.

References

1 Prohl, M. A., "A Method for Calculating Vibration Frequency and Stress of a Banded Group of Turbine Buckets," TRANS. ASME, Vol. 80, 1958, pp. 169–180.

2 Weaver, F. L., and Prohl, M. A., "High-Frequency Vibration of Steam-Turbine Buckets," TRANS. ASME, Vol. 80, 1958, pp. 181–194.

3 Kemp, N. H., and Sears, W. R., "Aerodynamic Interference Between Moving Blade Rows," *Journal of the Aerospace Sciences*, Vol. 20, No. 9, Sept. 1953, pp. 585–597 and 612.

4 Kemp, N. H., and Sears, W. R., "The Unsteady Forces Due to Viscous Wakes in Turbomachines," *Journal of the Aerospace Sciences*, Vol. 22, No. 7, July 1955, pp. 478–483.

5 Mayer, R. X., "The Effect of Wakes on the Transient Pressure and Velocity Distribution in Turbomachines," TRANS. ASME, Vol. 80, 1958, pp. 1544–1552.

6 Yeh, Hsuan, and Eisenhuth, J. J., "The Unsteady Wake Interaction in Turbomachinery and Its Effect on Cavitation," TRANS. ASME, *Journal of Basic Engineering*, Vol. 81, Series D, 1959, pp. 181–189.

7 Lefcort, M. D., "An Investigation Into Unsteady Blade Forces in Turbomachines," TRANS. ASME, *Journal of Engineering for Power*, Vol. 87, Series A, 1965, pp. 345–354.

8 Kolb, R. P., "Measured Vibratory Motions of Turbine Blades," ASME Paper No. 67-Vibr-66.

9 Pisarenko, G. S., "Vibrations of Elastic Systems Taking Account of Energy Dissipation in the Material" (transl. from Russian by Univ. of Minn.), Aeronautical Systems Div., Wright-Patterson AFB, Report No. WADD TR 60-582, Feb. 1962.

10 Hoerner, Sighard F., "Fluid-Dynamic Drag," published by the author, Midland Park, N. J., 1958.

11 Mori, Yasuo, "On Wakes Behind a Single Aerofoil and Cascade," *Bulletin of the Japan Society of Mechanical Engineers*, Vol. 2, No. 7, 1959, pp. 463–469.

12 Isay, W. H., "On the Potential Flow Through Airfoil Cascades" (in German), *Zeitschrift für Angewandte Mathematik und Mechanik*, Vol. 33, No. 12, Dec. 1953, pp. 397–409.

13 Bertolet, F. C., Westinghouse Steam Division, personal communication.

14 Lewis, F. M., "Propeller-Vibration Forces," *Trans. SNAME*, Vol. 71, 1963, pp. 293–326.

15 Giesing, J. P., "Nonlinear Interaction of Two Lifting Bodies in Arbitrary Unsteady Motion," *Journal of Basic Engineering*, TRANS. ASME, Series D, Vol. 90, No. 3, Sept. 1967, p. 387.

16 Horlock, J. H., "Fluctuating Lift Forces on Aerofoils Moving Through Transverse and Chordwise Gusts," *Journal of Basic Engineering*, TRANS. ASME, Series D, Vol. 90, No. 4, Dec. 1967, p. 494.

17 Lotz, M., and Raabe, J., "Blade Oscillations in One-Stage Axial Turbomachinery," *Journal of Basic Engineering*, TRANS. ASME, Series D, Vol. 90, No. 4, Dec. 1967, p. 485.